

# Determination of the Gelsolin Binding Site on F-actin: Implications for Severing and Capping

Amy McGough,\* Wah Chiu,\* and Michael Way#

\*Verna and Marrs McLean Department of Biochemistry, Baylor College of Medicine, Houston, Texas 77030 USA, and

#European Molecular Biology Laboratory, 69117 Heidelberg, Germany

**ABSTRACT** Gelsolin is a six-domain protein that regulates actin assembly by severing, capping, and nucleating filaments. We have used electron cryomicroscopy and helical reconstruction to identify its binding site on F-actin. To obtain fully decorated filaments under severing conditions, we have studied a derivative (G2-6) that has a reduced severing efficiency compared to gelsolin. A three-dimensional reconstruction of G2-6:F-actin was obtained by electron cryomicroscopy and helical reconstruction. The structure shows that gelsolin bridges two longitudinally associated monomers when it binds the filament. The F-actin binding region of G2-6 is centered axially at subdomain 3 and radially between subdomains 1 and 3 of the upper actin monomer. Our results suggest that for severing to occur, both gelsolin and actin undergo large conformational changes.

## INTRODUCTION

Gelsolin (Yin and Stossel, 1979) is the best-characterized member of a family of actin-binding proteins that includes severin, villin, fragmin, adseverin, and scinderin (reviewed in Matsudaira and Janmey, 1988; Weeds and Maciver, 1993). It is composed of six homologous domains, which are related in sequence, termed G1-6 (Kwiatkowski et al., 1986; Way and Weeds, 1988). In the presence of calcium, gelsolin severs and caps actin filaments. Alternatively, gelsolin can nucleate actin filament polymerization by lowering the critical concentration required for filament assembly by binding two actin monomers (Bryan and Kurth, 1984; Ditsch and Wegner, 1994). These diverse activities make gelsolin a powerful cellular regulator of actin's function in cells (Stossel, 1994a). In addition to its importance in living cells (Finidori et al., 1992; Witke et al., 1995; Arora and McCulloch, 1996; Lu et al., 1997; Ohtsu et al., 1997), gelsolin has been demonstrated to be an effective mucolytic agent for cystic fibrosis (CF) sputum and is currently in clinical trials as a therapeutic agent for CF (Vasconcellos et al., 1994; Stossel, 1994b; Sheils et al., 1996; Biogen Annual Report, 1995).

Filament severing by gelsolin may be modeled as a multistep process (Way et al., 1989; Kinosian et al., 1996). The first step in severing is binding to an as yet undetermined site on the actin filament. This is accomplished by the second domain of gelsolin (G2) and is a relatively slow step (Way et al., 1992; Allen and Janmey, 1994). After binding, gelsolin rapidly severs F-actin and then remains bound to

the barbed end of one of the newly formed filaments, forming a stable cap (Bryan and Kurth, 1984). Capping and severing are also regulated by specific interactions between gelsolin and phosphatidylinositol phosphate (PIP) or phosphatidylinositol 4,5-bisphosphate (PIP<sub>2</sub>) (Janmey and Stossel, 1987; Janmey et al., 1992).

Analysis of genetically engineered fragments of gelsolin has shown that domains G1 and G2 are sufficient for efficient filament severing and capping (Way et al., 1992). Domains G4-6 confer calcium sensitivity on severing and are required to nucleate polymerization (Way et al., 1989). Thus, in total, gelsolin contains three actin-binding sites: two monomer-binding sites (G1 and G4) and one filament-binding site (G2) (Bryan, 1988; Weeds and Maciver, 1993; Way et al., 1989, 1992; Pope et al., 1995). The functions of the other domains (G3, G5, and G6) are not clear.

Despite the growing body of structural data on this family of proteins (McLaughlin et al., 1993; Markus et al., 1994; Schnuchel et al., 1995; Burtnick et al., 1997), there is still no direct information on how gelsolin interacts with F-actin. Because gelsolin severs filaments very rapidly, we cannot directly study the interactions that occur during the severing process. As an alternative, we have performed electron cryomicroscopy of F-actin decorated with G2-6, a gelsolin deletion mutant that lacks the high-affinity monomer-binding domain that is required for efficient severing (Way et al., 1989). In EGTA, gelsolin G2-6 binds to filaments through domains G2-3 but does not sever. However, in calcium the C-terminal half (G4-6) can also bind actin, resulting in filament severing. The inefficient severing by G2-6 (17% that of gelsolin; Way et al., 1989) offers the possibility of "freezing" the severing mechanism in action, a feat that would be technically impossible with full-length gelsolin. Thus, in addition to allowing us to directly identify for the first time the binding site for G2-3 on the filament, the G2-6:F-actin structure should provide insights into how gelsolin severs and caps filaments.

Received for publication 21 August 1997 and in final form 11 November 1997.

Address reprint requests to Dr. Amy McGough, Department of Biochemistry, Baylor College of Medicine, Houston, TX 77030. Tel.: 713-798-6989; Fax: 713-796-9438; E-mail: amcgough@bcm.tmc.edu.

© 1998 by the Biophysical Society

0006-3495/98/02/764/09 \$2.00

## METHODS

### Electron cryomicroscopy

G2-6 and G2-3 were expressed and purified from *Escherichia coli* as described previously (Way et al., 1989, 1992). F-actin (2  $\mu$ M) (Spudich and Watt, 1971) in 10 mM Tris, 50 mM NaCl, 1 mM MgCl<sub>2</sub>, 1 mM dithiothreitol, 0.2 mM ATP, pH 7.8 ("F-actin buffer"), containing 0.5 mM CaCl<sub>2</sub> was gently mixed with a 4–5 molar excess of G2-6 in F-actin buffer containing 1 mM CaCl<sub>2</sub> and then plunged within 1 min. Approximately 7  $\mu$ l of filaments was placed on 400-mesh copper grids prepared with holey carbon films, blotted with filter paper, rapidly frozen in ethane slush cooled with liquid nitrogen, and maintained in liquid nitrogen until used. Samples were also pelleted for 15 min at 100,000 g in a Beckman airfuge and sodium dodecyl sulfate–polyacrylamide gel electrophoresis gels run to confirm gelsolin binding to actin. In some cases F-actin was decorated by applying 5  $\mu$ M G2-6 in calcium to actin filaments that had already been applied to an electron microscope grid. G2-3:F-actin filaments were prepared by incubating F-actin with a 4–5 molar excess of G2-3 for 30–90 min on ice in F-actin buffer containing 0.5 mM CaCl<sub>2</sub>. Images (100 KeV) of F-actin, G2-3:F-actin, and G2-6:F-actin in calcium were recorded at a nominal magnification of 30,000 $\times$  and 2.6–3.3  $\mu$ m underfocus with a JEOL 1200 electron cryomicroscope (McGough and Way, 1995; McGough et al., 1997). Images of G2-6:F-actin in F-actin buffer containing 0.2 mM EGTA were recorded at  $\sim$ 1.0–1.5  $\mu$ m underfocus on a Philips CM12 electron cryomicroscope operated at 120 KeV (McGough et al., 1994).

### Structure determination, analysis, and visualization

Electron micrographs were scanned on a Perkin-Elmer densitometer at 5.3  $\text{\AA}$  per pixel. The defocus of the micrographs used for the structural analysis was determined by incoherent averaging of calculated diffraction patterns obtained from either regions of adjacent carbon or protein embedded in ice (Zhou et al., 1996). Helical reconstructions were performed using PHOENIX run on a Silicon Graphics workstation (DeRosier and Moore, 1970; Schroeter and Bretaudiere, 1996; Whittaker et al., 1995a). Alignments were performed using the layer lines indicated by the following  $n, l$  values: (2, 1), (4, 2), (–5, 4), (–3, 5), (–1, 6), (1, 7), and (3, 8). All data points along the layer lines (excluding those at the meridian) up to a resolution of 1/37  $\text{\AA}^{-1}$  were used in the alignments.

A total of 54 G2-6:F-actin filaments (out of 110 filaments analyzed) were successfully aligned to a reference data set after three rounds of alignment. We found that as more G2-6:F-actin filaments were included in the average, the high radius features (which corresponded to the G2-6) had a tendency to weaken. To resolve as much of the G2-6 density as possible, we tried various schemes for deciding which filaments to incorporate into the final average. The approaches tried included using only those data sets with the best phase residuals, the greatest differences between up/down phase residuals, and the best agreement of the relative shifts between sides, and those corresponding to the side of the particle giving the lowest phase residuals. Even with such approaches, which were designed to select for the best-preserved particles, the averaged images remained essentially the same. The decrease in the intensity of the arm suggests that not all 54 filaments included in the average have this high radius feature; however, diffraction patterns and layer-line data of individual G2-6:F-actin filaments do not show readily apparent differences. In contrast, in real space the presence or absence of the arm is readily apparent from visual inspection of the reconstructed particles. Therefore, visual inspection of projection maps derived from three-dimensional reconstructions of individual sides was used to help prescreen the filaments for inclusion in the average. We used only those filaments whose phase residuals fell within the lower half of the population and performed a running average of the filaments. Averaging was stopped when inclusion of an additional filament was found to weaken, rather than strengthen, the arm. A similar approach was required to resolve the "off" position of tropomyosin, owing to disorder in the tropomyosin strands on thin filaments (Vibert et al., 1993). This earlier

study on thin filaments differs from our present study in that additional screening was possible from the raw images because their specimen was negatively stained.

The gelsolin G2-6 portion of the map was identified by difference mapping. The phase residuals calculated for the final G2-6:F-actin reconstruction (average of 15 data sets) when aligned against the F-actin reconstruction (average of 16 data sets) were 39.9° and 51.5° for the correct and incorrect polarities, respectively. The polarity of the actin filaments was determined by comparison to a reconstruction of actoS1 (Whittaker et al., 1995b). The difference map in Fig. 4 *d* was computed by multiplying the reconstruction with a binary mask (Schroeter and Bretaudiere, 1996) derived from the F-actin reconstruction. The difference map in Fig. 4 *e* was calculated by subtracting the F-actin densities from the G2-6:F-actin densities and contouring the positive differences (McGough et al., 1994). The significance of the differences was assessed by computing statistical difference maps (Milligan and Flicker, 1987). The region of the reconstruction that we have designated G2-3 was highly statistically significant ( $p < 0.00005$ ) according to this criterion. The high radius densities were less significant, but it was still a stronger density than the surrounding noise (one standard deviation above the mean density of the map).

Atomic models and density maps were displayed and manipulated using IRIS Explorer (Numerical Algorithms Group) and O version 5.9 (Jones et al., 1991). Alignment of the atomic model of F-actin proposed by Lorenz et al. (1993) was done interactively by rigid body translation and rotation to the molecular envelopes determined by electron microscopy reconstructions. Ribbon diagrams were generated using Ribbons 2.65 (Carson and Bugg, 1986), saved as Inventor format files, and displayed in IRIS Explorer.

## RESULTS

### Appearance of G2-6 decorated actin filaments

The most widely studied F-actin-binding protein, myosin, binds actin tightly and reduces the helical disorder inherent in the filament (Stokes and DeRosier, 1987). This leads to a strongly diffracting structure that is amenable to study by standard approaches. In contrast, the F-actin-binding domain of gelsolin binds weakly ( $K_d = 2\text{--}4 \mu\text{M}$ ; Way et al., 1992), and gelsolin G2-6 destabilizes (severs) the actin filament. These properties had to be taken into consideration during our study. To achieve saturation of the filaments, we incubated F-actin with a 4–5 molar excess of G2-6. As a result of the excess protein, electron micrographs of G2-6:F-actin filaments (Fig. 1 *a*) possess high levels of noise. We also observed that under these conditions the filaments varied widely in length relative to equivalent preparations of F-actin alone (Fig. 1 *b*) or decorated with either G2-6 in EGTA (Fig. 1 *c*) or G2-3 in calcium (Fig. 1 *d*). Presumably many of the shorter filaments had been severed by G2-6 during the time it took to prepare the grids for electron microscopy.

In addition to the length variation, many of the G2-6:F-actin filaments were kinky or curvy. In contrast, actin filaments either alone or combined with G2-6 in EGTA or with G2-3 in calcium are usually either straight or show only gradual bending. Because decoration by most actin-binding proteins results in stabilization rather than distortion of filament structure (Milligan and Flicker, 1987; Vibert et al., 1993; Owen and DeRosier, 1993; McGough et al., 1994), it is likely that the kinking we have observed is related to the severing activity of G2-6 (Way et al., 1989).

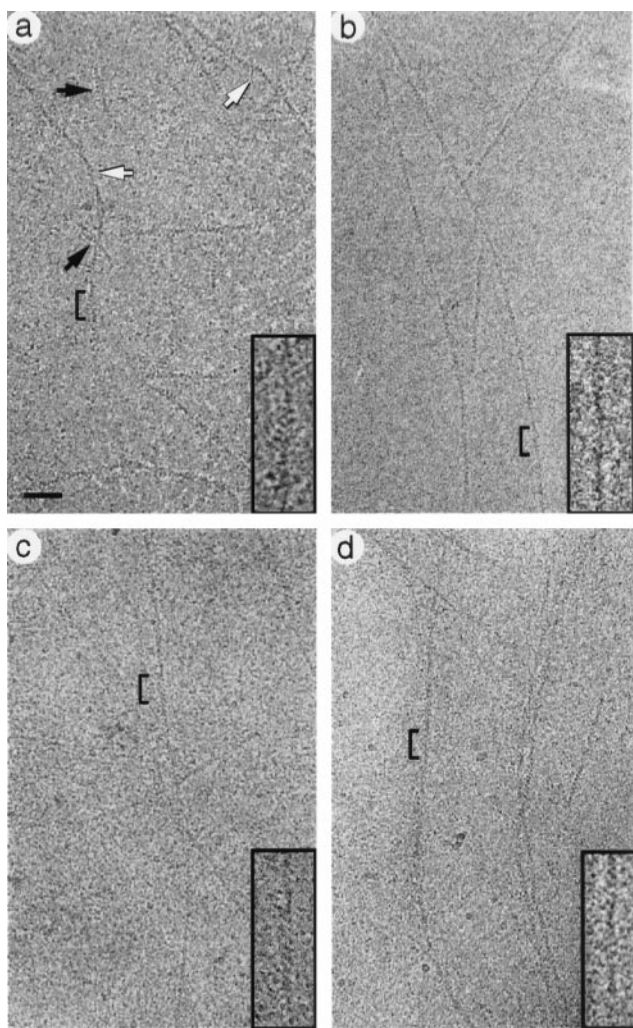


FIGURE 1 Electron cryomicrographs of (a) G2-6:F-actin in calcium, (b) F-actin, (c) G2-6:F-actin in EGTA, and (d) G2-3:F-actin in calcium. Brackets indicate one cross-over on a filament. Insets contain enlargements of filaments showing three cross-overs. Black arrowheads indicate short actin filaments, and white arrowheads indicate kinky filaments in a. Both types of filaments are commonly found under severing conditions. The G2-6:F-actin filaments in b are of lower contrast, owing to the imaging conditions used to produce this micrograph. Protein is dark in these images. Bar = 500 Å.

Even in these noisy micrographs it is usually possible to discern by eye that the G2-6:F-actin filaments are wider than F-actin alone. Often the presence of “arms” extending out from the filament can be identified in the raw images (see *inset*, Fig. 1 a). To determine their structure, we calculated diffraction patterns from computationally straightened filaments (Fig. 2). The diffraction patterns show layer lines characteristic of the actin helix. The mean helical symmetries for the G2-6:F-actin and F-actin filaments included in the final reconstructions were 2.1621 ( $\sigma = 0.0081$ ) and 2.1625 ( $\sigma = 0.0012$ ) subunits/turn, respectively, indicating that the G2-6:F-actin filaments exhibit a larger variation in helical twist relative to bare F-actin. This may be due to the distortion in the filaments induced by

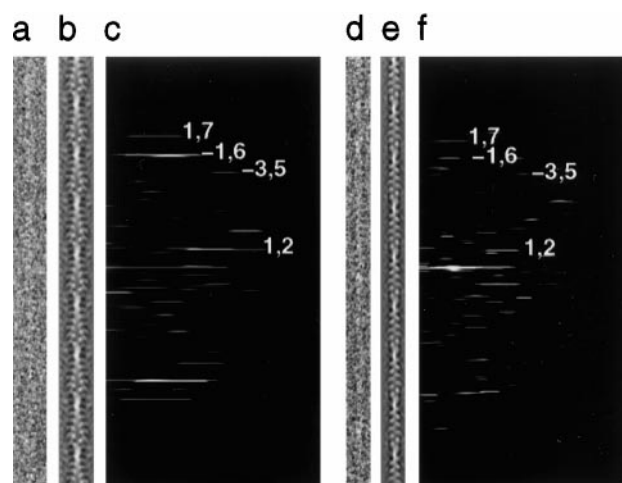


FIGURE 2 Computationally straightened images, projection maps, and computed diffraction patterns of (a–c) G2-6:F-actin in calcium and (d–f) F-actin. Images show equivalent length portions of computationally straightened filaments and are best viewed from a glancing angle. The actual lengths of the filaments used to calculate the diffraction patterns were 0.88 and 0.55  $\mu\text{m}$  for a and c, respectively. Protein is light in these images. Layer lines are labeled with values of  $n$  and  $l$ .

gelsolin G2-6 under these severing conditions. The mean twist of the G2-6:F-actin filaments, however, was unchanged. This is in contrast to another F-actin-fragmenting protein, cofilin, which has recently been reported to substantially alter the mean twist of the filament (McGough et al., 1997).

### Reconstruction of G2-6:F-actin under conditions that permit severing

Because F-actin is a helical object, its three-dimensional structure can be determined directly from the layer-line data of individual filaments. A three-dimensional reconstruction obtained from the single G2-6:F-actin filament shown in Fig. 2 a is shown as a projection map in Fig. 2 b. The image reveals bent “arms” that approximately double its diameter relative to F-actin (Fig. 2 e). It is important to note that this reconstruction represents an average consisting of the 180 G2-6:actin subunits that form the filament. This internal averaging produces a dramatic improvement in image quality and interpretability relative to the raw image from which it was obtained.

We sought to improve further the signal-to-noise ratio and reliability of the structures by additional averaging. Accordingly, layer-line data from eight G2-6:F-actin or F-actin filaments were aligned and averaged to produce the final reconstructions. The mean phase residuals for the final G2-6:F-actin and F-actin reconstructions were 42.4° and 27.1°, respectively. These phase residuals are comparable to those reported for other actin structures calculated in a similar way (that is, calculated using the entire layer lines rather than just the peaks; McGough et al., 1994; Owen and DeRosier, 1993). The higher phase residual obtained for the

decorated filaments is probably a function of the contribution of free G2-6 to the background as well as of disorder in the filaments themselves. The up-down differences in phase residuals were  $15.9^\circ$  for the G2-6:F-actin structure and  $20.8^\circ$  for the F-actin structure.

Fig. 3 presents plots of amplitudes and phases for the two averaged data sets. Both the diffraction patterns and layer-line data of the decorated filament show relative increases in layer lines 1, 4, and 7, as well as shifting the peaks along layer lines toward the meridian. The latter is consistent with the increase in particle diameter of G2-6:F-actin. The increase in the intensity of layer line 1, and to a lesser extent layer line 2, is consistent with the enhanced appearance of the actin “cross-overs” that arise from the two-stranded long-pitched actin helix (compare Fig. 2 *b* with 2 *e*).

Three-dimensional reconstructions were calculated by Fourier-Bessel inversion of averaged layer-line data. The G2-6:F-actin filament (Fig. 4 *a*) is  $\sim 175$  Å in diameter or nearly double the diameter of F-actin. The bulky region of the arm is tilted up, resulting in a filament polarity that is opposite that of myosin S1 decorated filaments. The reconstruction may be more readily interpreted by comparison with a reconstruction of F-actin obtained under comparable conditions (*white filament* in Fig. 4 *b*). Our interpretation of the reconstruction is that G2-6 binds at the junction between two actin monomers and extends out across the front of the filament (in a clockwise direction when looking down the pointed end of actin).

The weakest region of the map occurs most distal from the filament binding site. We found that as more filaments were included in the average, the high-radius features were weakened, whereas the low-radius mass touching the actin filament remained essentially unchanged. Comparison of a reconstruction of G2-6:F-actin based on 54 filaments (Fig. 4 *c*) with the final reconstruction containing data from eight filaments (Fig. 4 *a*) shows that the portion of G2-6 that is directly bound to F-actin is a stable feature, even with additional averaging. The extended arms, which are clearly visible in the eight-filament average, on the other hand,

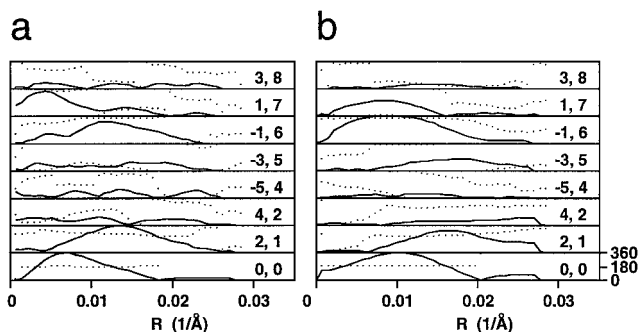


FIGURE 3 Plots of  $G_n I(R)$  (—) amplitudes and (.....) phases (Klug et al., 1958). (a) Average layer-line data from eight G2-6:F-actin filaments. (b) Average layer-line data from eight F-actin filaments. The order and layer-line number ( $n$ ,  $l$ ) are listed for each layer line. Amplitudes are scaled relative to the strongest nonequatorial layer line for each filament; equators are on their own scale. Phases vary from  $0^\circ$  to  $360^\circ$ .

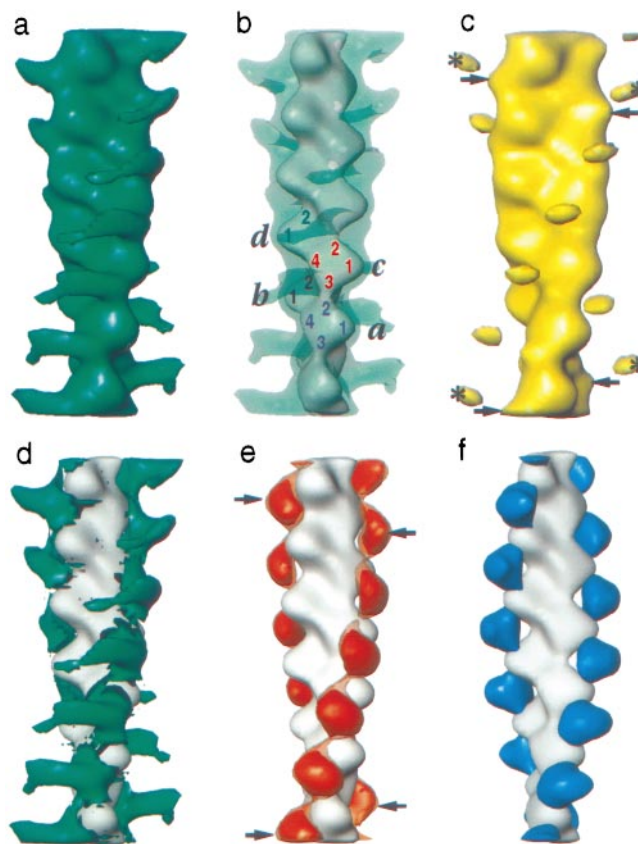


FIGURE 4 Identification of the F-actin binding site by difference mapping. (a) Surface rendering of final G2-6:F-actin reconstruction based on eight filaments or  $\sim 1220$  G2-6:actin subunits (green) contoured at  $1\sigma$ . This corresponds to 110% of the predicted molecular volume, assuming a 1:1 ratio of actin to G2-6. Lowering the contour level below  $1\sigma$  introduced floating noise into the map. (b) F-actin reconstruction (white), obtained under similar conditions, embedded in the G2-6:F-actin reconstruction (transparent green). Four monomers in the filament (a–d) and the approximate positions of the four subdomains of actin (Kabsch et al., 1990; Holmes et al., 1990) are indicated. (c) Preliminary G2-6:F-actin reconstruction calculated from 54 filaments or  $\sim 6700$  G2-6:actin subunits (yellow). Asterisks indicate the position of a small volume of density in the preliminary map, which coincides with the “arms” visible in the final reconstruction. Arrowheads indicate the positions of the low radius masses that coincide with the F-actin binding component of gelsolin. (d) F-actin displayed with the difference map (green) obtained by masking out F-actin from the final G2-6:F-actin reconstruction. (e) F-actin displayed with a difference map (transparent orange) contoured to account for the molecular mass of the F-actin binding fragment G2-3. The statistical difference map (opaque orange) is contoured to a significance level of  $p < 0.00005$ . (f) F-actin displayed with the actin binding domain of  $\alpha$ -actinin, shown in blue (McGough et al., 1994).

become much weaker with additional averaging. The next strongest feature in the map calculated from 54 filaments is a smaller density at high radius, which coincides with the position of the G2-6 arms and which we interpret as a feature of the G2-6 arms remaining after averaging.

Because there is always some ambiguity in assigning the precise boundary separating the particle from the embedding medium (Frank, 1996), which is a prerequisite for generating the 3D models shown in Fig. 4, we have also

assessed the behavior of the high-radius features from projection maps. Comparison of the projections calculated from reconstructions of a single filament, an eight-filament average, and a 54-filament average leads to the same conclusions (Fig. 5).

Two factors that would contribute to the sensitivity of features distal from the filament-binding site to additional averaging are flexibility in G2-6 at the junction between the F-actin (G2-3) and the G-actin (G4-6) binding halves of the molecule and/or different conformational states of G2-6, both on the same filament and between filaments. The fact that some filaments are long and straight, some are kinky, and others are very short leads us to believe that different G2-6 molecules are at different stages in the mechanism and possibly in different conformations as well. In either case, it is clear from the average of 54 filaments that the portion of gelsolin G2-6 that is directly attached to actin (which must therefore contain the F-actin-binding domain) is a stable feature.

### Identification of the gelsolin-binding site on F-actin by difference mapping

To isolate the gelsolin component of the reconstruction, we computed difference maps after aligning the G2-6:F-actin and F-actin structures in Fourier space. The difference map shown in Fig. 4 *d* was calculated by carving out the actin filament from the G2-6:F-actin filament, using a binary mask derived from the F-actin reconstruction. This exercise confirms that each G2-6 extends out from the gaps between two longitudinally associated actin subunits in the filament. The size of the arm corresponds to ~74% of the volume predicted for G2-6, based on its molecular mass. The underrepresentation of the gelsolin in our reconstruction is probably a function of the limited resolution of the reconstruction, partial decoration of the filament, and disorder in the molecule.

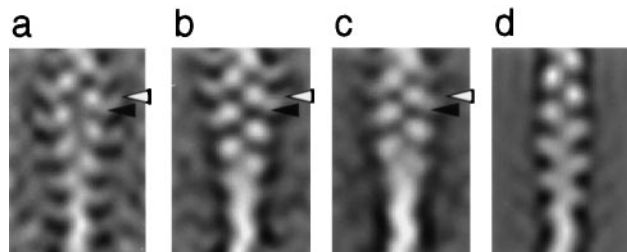


FIGURE 5 Averaging of G2-6:F-actin and F-actin filaments. The effects of averaging layer-line data from (a) a single filament, (b) eight filaments, and (c) 54 filaments on projection images of G2-6:F-actin reconstructions. Averaging was stopped after eight filaments because it was apparent that additional averaging was weakening the high radius features (black arrowheads), which are visible in *a* and *b*. Black arrowheads indicate the low radius mass, which is a constant feature in the G2-6 decorated filaments, even after many filaments are averaged together. (d) F-actin reconstruction based on eight filaments, viewed as a projection image for comparison. Protein is light in these images.

Fig. 4 *e* shows difference maps calculated using two alternative approaches that highlight the strongest differences between the two maps. The transparent orange densities were calculated by subtracting the F-actin map as continuous densities from the G2-6:F-actin map. It is shown contoured to occupy the molecular volume predicted for G2-3. The statistical difference map or “t map” (Milligan and Flicker, 1987) is presented in opaque orange on the same filament. It is shown contoured at a significance level of  $p < 0.00005$ , indicating that the low-radius mass that is bound to F-actin is highly reliable.

## DISCUSSION

### Gelsolin binding to the actin filament

Despite the extensive study that has been made over the past two decades of gelsolin and its relatives, there is little structural information on how gelsolin binds to and severs actin filaments. The first goal of this study was to determine the gelsolin-binding site on the actin filament. The maps presented in Fig. 4 show that gelsolin G2-6 binds the filament by interactions with two actin monomers, in support of the model for F-actin binding that was first proposed by Pope et al. (1991). The most extensive interactions appear to involve the upper monomer. The gelsolin-binding site on F-actin is centered axially at subdomain 3 and radially between subdomains 1 and 3 of the upper monomer. Subdomains 1 and 2 of the lower monomer also appear to be involved in the gelsolin-binding site.

Immunochemical studies have identified regions of subdomain 1 of actin (residues 1–10 and 18–28) as important for G2 binding (Feinberg et al., 1995). The involvement of actin residues 23–28 with gelsolin binding is consistent with the interactions we see in our structure (see Fig. 6). However, our reconstruction and difference mapping suggest that the amino terminus is not located directly in the gelsolin-binding site. This discrepancy is not too surprising, because the amino-terminal residues of actin are thought to be highly mobile (Kabsch et al., 1990). In earlier studies of  $\alpha$ -actinin’s interactions with F-actin, the amino-terminal residues were also thought to be involved in binding (Mimura and Asano, 1987), only to be shown later to fall outside the binding site (see Fig. 4 *f*; McGough et al., 1994).

In some places the positive densities from the difference maps appear to contact one another along the long-pitched helix of the actin filament. These connections are extremely sensitive to the contour level used to represent the map and are probably a result of the low resolution of the G2-6:F-actin reconstruction. Therefore, it is unlikely that the G2-6 molecules make contact with each other when bound to the filament. This is in agreement with binding studies showing that filament binding by G2-3 and G2-6 is not cooperative, as might be expected if adjacent molecules along the filament were touching (Way et al., 1992).

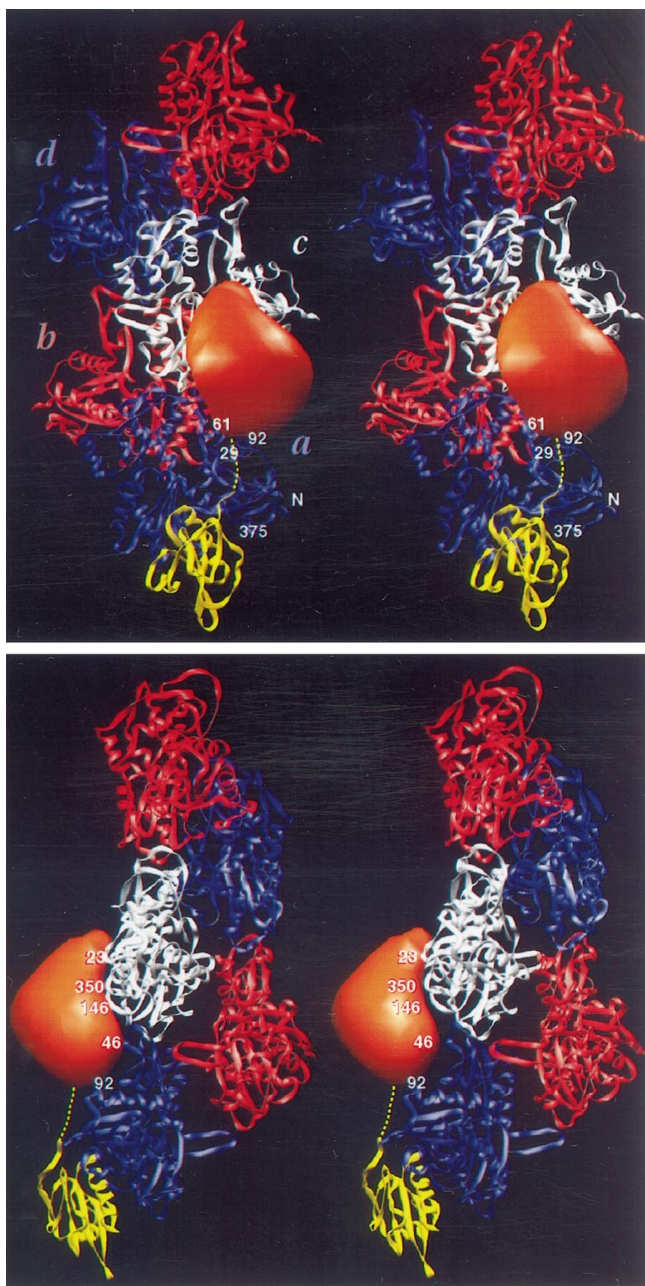


FIGURE 6 Model of an actin filament capped with gelsolin G1-3. Five subunits in the Lorenz model of F-actin (Lorenz et al., 1993) are shown in stereo at two different orientations. The model was generated by interactively fitting the Lorenz model of F-actin into the G2-6:F-actin and F-actin reconstructions, then combining this model of F-actin binding with the atomic model of G1 bound to G-actin (McLaughlin et al., 1993). According to this model, the G1-3 cap involves monomers a and c. A dashed line is used to indicate the residues that bind PIP2 and connect domains G1 and G2. The images are designed to be viewed with a stereo viewer.

### Relationship to other F-actin-binding proteins

Electron microscopy has been used to determine the filament-binding sites of a variety of actin-binding proteins, including myosin, tropomyosin, scruin,  $\alpha$ -actinin, and cofilin. The gelsolin-binding site appears to overlap the sites for myosin (Rayment et al., 1993; Schroder et al., 1993), scruin

(Owen and DeRosier, 1993; Schmid et al., 1994), and cofilin (McGough et al., 1997). Unfortunately, there are no data available on competition between gelsolin and these proteins for filament binding. However, based on its binding site, we predict that gelsolin would compete with these proteins for filament binding. The location of G2-6 on the actin filament is consistent with the inhibitory effects of tropomyosin and caldesmon on severing by gelsolin, as well as with the placement of tropomyosin on the actin filament (Dabrowska et al., 1996; Vibert et al., 1993; Hodgkinson et al., 1997).

Interestingly, the G2-6 binding site on F-actin is quite similar to that of  $\alpha$ A1-2, the actin-binding domain of  $\alpha$ -actinin (Fig. 4 *f*), even though these two proteins are unrelated in both sequence and function. This is consistent with the finding that  $\alpha$ A1-2 can both substitute functionally for G2-3 during severing and compete with G2-3 for filament binding (Way et al., 1992). These results, taken together with the facts that G2-3 contains the F-actin-binding domain (Yin et al., 1988; Bryan, 1988) and calcium-dependent actin binding by G4-6 (after targeting to the filament by G2-3) results in severing (Way et al., 1989), lead us to argue that the difference density shown in Fig. 4 *e* corresponds to all or part of G2-3.

To date, all F-actin-binding proteins have been found to interact with at least two subunits in the filament. In most cases these interactions involve two or more longitudinally associated subunits. This suggests that specificity for filamentous rather than monomeric actin is a direct consequence of binding two or more subunits that are related by the relatively restricted geometry accommodated by the F-actin helix. Thus filament geometry may be just as important in defining binding sites as the specific amino acid residues that are involved in the interactions.

### Structural model for the basis of filament distortion during severing

In addition to showing how gelsolin binds the actin filament, our structure of G2-6:F-actin obtained in calcium holds the potential of visualizing the domains that are responsible for severing by G2-6, as well as providing insights into the severing mechanism. Given that G2-3 contains the filament-binding site and subsequent calcium-dependent actin binding by G4-6 results in severing, we propose that G4-6 is the source of the remaining high-radius density, which trails off in the clockwise direction across the front of the filament.

Because G4-6 on its own does not bind F-actin, we cannot determine its structure when bound directly to actin by helical reconstruction methods. However, existing biochemical and structural data on gelsolin/actin interactions, combined with our structure, allow us to propose how G4-6 binds the filament when severing is completed (Fig. 7). Biochemical and structural studies suggest that G4 binds at the base of the actin monomer in a position similar to that of

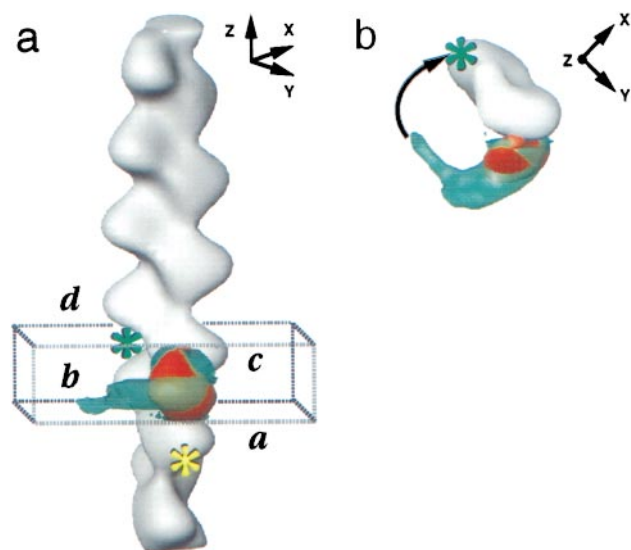


FIGURE 7 Mechanistic model of domain movements required for G2-6 to sever F-actin. (a) A single G2-6 molecule is bound to actin subunits a and c. The top of the filament is tilted toward the reader at a small angle for clarity. Domain assignments are derived from reconstructions coupled with existing biochemical data on gelsolin's interactions with actin. The G1 binding site is indicated with a yellow asterisk. The closest available G4 binding site is at the base of monomer d and is indicated with a green asterisk. (b) View down the filament, consisting of the region enclosed by the dashed box. The large conformational change needed to bring gelsolin in proximity to the G4 binding site is particularly evident in the end view, as indicated by the arrow.

G1 (Pope et al., 1991; McLaughlin et al., 1993; Pope et al., 1995; Burtnick et al., 1997). Although the individual domains are not resolved in this reconstruction, the position of the G2-6 arm suggests that the closest available binding site for G4 would be between 50 Å and 100 Å away, at the base of monomer d. This suggests that gelsolin undergoes dramatic conformational changes in calcium for G4 to bind actin and sever the filament. In support of this proposal, it is known that the hydrodynamic volume of gelsolin doubles (Patowski et al., 1990) and assumes a more asymmetrical shape (Rouayrenc et al., 1986), and dynamic light scattering experiments indicate that domains G4-6 undergo major conformational changes upon binding calcium (Hellweg et al., 1993).

In addition to the proposed conformational change in gelsolin, we have observed substantial distortions in actin filaments decorated with G2-6 under conditions that permit severing (Fig. 1 a). Filament distortions have also been observed by video-enhanced light microscopy of full-length gelsolin severing F-actin (Bearer, 1991). The G2-6:F-actin reconstruction provides a structural explanation for these observations. Given the sizes of the domains involved and the distance between the filament-binding site and the nearest available G4-binding site, an additional conformational change may also be required within actin during severing. Assuming that all three actin-binding domains remain bound to F-actin after severing, it is likely that, in addition to distortions in actin that might occur during severing, the

subunits at the end of the gelsolin-capped filament would also be distorted. Consistent with this notion, alterations of actin structure, when present in ternary complexes with gelsolin, have been observed by a number of biochemical and biophysical techniques (Hesterkamp et al., 1993; Prochniewicz et al., 1996; Khaitlina and Hinssen, 1997) and electron microscopy (Orlova et al., 1995). According to our model, the gelsolin cap would involve direct interactions with three actin monomers (labeled a, c, and d in Fig. 6).

### Efficient versus inefficient severing

The gelsolin derivative G1-3 has been shown to sever F-actin very efficiently *in vitro* (Chaponnier, 1986; Way et al., 1989). This raises the question of the roles of domains 4–6 in gelsolin. Although it is clear that these domains are important for calcium regulation, it seems evolutionarily inefficient for half of gelsolin's molecular mass to be devoted to calcium regulation when other proteins accomplish the same feat with much smaller domains. Unfortunately, the speed with which G1-3 severs makes structural studies of this protein in association with F-actin unfeasible. Our reconstruction of G2-6:F-actin filaments clarifies the roles of both G2-3 and G4-6 during severing and leads us to propose the following mechanisms for severing by G1-3 and G2-6.

We have found that gelsolin's F-actin-binding domain bridges two longitudinally associated monomers in the filament. Because G1 does not sever F-actin on its own, filament recognition by G2 is the first, critical step in severing. We propose that in the absence of PIP<sub>2</sub>, the junction between G1 and G2 is flexible, and G1, which is now tethered to the filament by G2-3, rapidly finds its binding site. In this scheme for filament severing by G1-3, G2-3 steers G1 into position, then G1 drives a wedge between longitudinally associated actin monomers and breaks the filament. After severing by G1-3, one of the newly formed filaments is capped at its barbed end. Fig. 6 presents a model of the filament capped with G1-3. The model shows that a G1-3 cap would involve two actin subunits related by the long-pitch helix of the filament. This is consistent with biochemical evidence showing that G1-3 binds two actins (Bryan and Hwo, 1986; Way et al., 1989), as well as with our reconstruction showing G2-6 associated with two subunits along the long-pitch actin helix.

Does the importance of G2-3 and G1 mean that G4-6 does not play a role during severing? *In vitro* severing assays have demonstrated that G1-3 and G2-6 sever filaments at ~87% and 17% the efficiency of gelsolin, respectively (Way et al., 1989). A major contributing factor to the differences in the way G1-3 and G2-6 sever is that G1 binds monomeric actin with 1000-fold greater affinity than G4-6 (Bryan, 1988). For this reason, it appears that an additional element in the mechanism is required for G2-6 to sever the filament. We propose that the dramatic distortions seen in our electron cryomicrographs of G2-6:F-actin filaments

provide this driving force. These distortions are reminiscent of, although distinct from, the substantial change in helical twist produced by the F-actin-fragmenting protein cofilin (McGough et al., 1997). Further studies will be needed to determine if G2-6 is actively or passively producing these distortions and if filament distortion is a component of all severing mechanisms. In conclusion, the G2-6:F-actin reconstruction presented here provides the first direct structural data on how gelsolin binds the actin filament and suggests that, in addition to its importance in calcium regulation and nucleation, domains G4-6 may play an important role during severing.

We thank D. DeRosier (Brandeis University), B. Pope and A. Weeds (MRC-LMB), L. Orlova (Imperial College), M. Sherman (Baylor College of Medicine), and P. Thuman-Commike (Rice University) for helpful discussions; R. Edwards (Baylor College of Medicine) for the generous gift of actin; and R. Diaz (Florida State University) and B. Carragher and D. Weber (Beckman Institute) for help with software. AM thanks D. DeRosier (National Institutes of Health, GM26357), and MW thanks Paul Matsudaira for support during the initial stages of this work.

This research was supported by a grant-in-aid from the American Heart Association (to AM), a grant from National Institutes of Health (RR02250 to WC), and the W. M. Keck Center for Computational Biology (Houston, TX). During earlier stages of this work, AM was supported by either an National Institutes of Health National Research Service Award postdoctoral fellowship (AR08207-03) or a training grant from the National Library of Medicine (1T15LM07093).

## REFERENCES

- Allen, P. G., and P. A. Janmey. 1994. Gelsolin displaces phalloidin from actin filaments. *J. Biol. Chem.* 269:32916–32923.
- Arora, P. D., and C. A. G. McCulloch. 1996. Dependence of fibroblast migration on actin severing activity of gelsolin. *J. Biol. Chem.* 271:20516–20523.
- Bearer, E. L. 1991. Direct observation of actin filament severing by gelsolin and binding by gCap39 and CapZ. *J. Cell Biol.* 115:1629–1538.
- Biogen Annual Report. 1995. Cambridge, MA. 3.
- Bryan, J. 1988. Gelsolin has three actin-binding sites. *J. Cell Biol.* 106:1553–1562.
- Bryan, J., and S. Hwo. 1986. Definition of an N-terminal actin-binding domain and a C-terminal  $\text{Ca}^{2+}$  regulatory domain in human brevin. *J. Cell Biol.* 102:1439–1446.
- Bryan, J., and M. C. Kurth. 1984. Actin-gelsolin interactions. Evidence for two actin-binding sites. *J. Biol. Chem.* 259:7480–7487.
- Burtnick, L. D., E. K. Koepf, J. Grimes, E. Y. Jones, D. I. Stuart, P. J. McLaughlin, and R. C. Robinson. 1997. The crystal structure of plasma gelsolin: implications for actin severing, capping and nucleation. *Cell.* 90:661–670.
- Carson, M., and C. E. Bugg. 1986. Algorithm for ribbon models of proteins. *J. Mol. Graph.* 4:121–122.
- Chaponnier, C., P. A. Janmey, and H. L. Yin. 1986. The actin filament-severing domain of plasma gelsolin. *J. Cell Biol.* 103:1473–1481.
- Dabrowska, R., H. Hinssen, B. Galazkiewicz, and E. Nowak. 1996. Modulation of gelsolin-induced actin filament severing by caldesmon and tropomyosin and the effect of these proteins on the actin activation of myosin  $\text{Mg}^{2+}$ -ATPase activity. *Biochem. J.* 315:753–759.
- DeRosier, D. J., and P. B. Moore. 1970. Reconstruction of three-dimensional images from electron micrographs of structures with helical symmetry. *J. Mol. Biol.* 52:355–369.
- Ditsch, A., and A. Wegner. 1994. Nucleation of actin polymerization by gelsolin. *Eur. J. Biochem.* 224:223–227.
- Feinberg, J., Y. Benyamin, and C. Roustan. 1995. Definition of an interface implicated in gelsolin binding to the sides of actin filaments. *Biochem. Biophys. Res. Commun.* 17:426–432.
- Finidori, J., E. Friederich, D. J. Kwiatkowski, and D. Louvard. 1992. In vivo analysis of functional domains from villin and gelsolin. *J. Cell Biol.* 116:1145–1155.
- Frank, J. 1996. Three-Dimensional Electron Microscopy of Macromolecular Assemblies. Academic Press, San Diego.
- Hellweg, T., H. Hinssen, and W. Eimer. 1993. The Ca-induced conformational change of gelsolin is located in the carboxy-terminal half of the molecule. *Biophys. J.* 65:799–805.
- Hestekamp, T., A. G. Weeds, and H. G. Mannherz. 1993. The actin monomers in the ternary gelsolin: 2 actin complex are in an antiparallel orientation. *Eur. J. Biochem.* 218:507–513.
- Hodgkinson, J. L., S. B. Marston, R. Craig, P. Vibert, and W. Lehman. 1997. Three-dimensional image reconstruction of reconstituted smooth muscle thin filaments: effects of caldesmon. *Biophys. J.* 72:2398–2404.
- Holmes, K. C., D. Popp, W. Gebhard, and W. Kabsch. 1990. Atomic model of the actin filament. *Nature.* 347:44–49.
- Janmey, P. A., J. Lamb, P. G. Allen, and P. T. Matsudaira. 1992. Phosphoinositide-binding peptides derived from the sequences of gelsolin and villin. *J. Biol. Chem.* 267:11818–11823.
- Janmey, P. A., and T. P. Stossel. 1987. Modulation of gelsolin function by phosphatidylinositol 4,5-bisphosphate. *Nature.* 325:362–364.
- Jones, T. A., J. Y. Zou, C. Cowan, and M. Kjeldgaard. 1991. Improved methods for the building of protein models in electron density maps and the location of errors in these models. *Acta Crystallogr.* A47:110–119.
- Kabsch, W., H. G. Mannherz, D. Suck, E. F. Pai, and K. C. Holmes. 1990. Atomic structure of the actin:DNase I complex. *Nature.* 347:37–44.
- Khaitlina, S., and H. Hinssen. 1997. Conformational changes in actin induced by its interaction with gelsolin. *Biophys. J.* 73:929–937.
- Kinosian, H. J., L. A. Selden, J. E. Estes, and L. C. Gershman. 1996. Kinetics of gelsolin interaction with phalloidin-stabilized F-actin. Rate constants for binding and severing. *Biochemistry.* 35:16550–16556.
- Klug, A., F. H. C. Crick, and H. W. Wycoff. 1958. Diffraction by helical structures. *Acta Crystallogr.* 11:199–213.
- Kwiatkowski, D. J., T. P. Stossel, S. H. Orkin, J. E. Mole, H. R. Colten, and H. L. Yin. 1986. Plasma and cytoplasmic gelsolins are encoded by a single gene and contain a duplicated actin-binding domain. *Nature.* 323:455–458.
- Lorenz, M., D. Popp, and K. Holmes. 1993. Refinement of the F-actin model against x-ray fiber diffraction data by the use of the directed mutation algorithm. *J. Mol. Biol.* 234:826–836.
- Lu, M., W. Witke, D. J. Kwiatkowski, and K. S. Kosick. 1997. Delayed retraction of filopodia in gelsolin null mice. *J. Cell Biol.* 138:1279–1287.
- Markus, M. A., T. Nakayama, P. Matsudaira, and G. Wagner. 1994. Solution structure of villin 14T, a domain conserved among actin-severing proteins. *Protein Sci.* 3:70–81.
- Matudaira, P. T., and P. A. Janmey. 1988. Pieces in the actin-severing puzzle. *Cell.* 54:139–140.
- McGough, A., B. Pope, W. Chiu, and A. Weeds. 1997. Cofilin changes the twist of F-actin: implications for actin filament dynamics and cellular function. *J. Cell Biol.* 138:771–781.
- McGough, A., and M. Way. 1995. Molecular model of an actin filament capped by a severing protein. *J. Struct. Biol.* 115:144–150.
- McGough, A., M. Way, and D. DeRosier. 1994. Determination of the  $\alpha$ -actinin binding site on actin filaments by cryoelectron microscopy and image analysis. *J. Cell Biol.* 126:433–443.
- McLaughlin, P. J., J. T. Gooch, H.-G. Mannherz, and A. G. Weeds. 1993. Structure of gelsolin segment 1-actin complex and the mechanism of filament severing. *Nature.* 364:685–692.
- Milligan, R. A., and P. F. Flicker. 1987. Structural relationships of actin, myosin, and tropomyosin revealed by cryo-electron microscopy. *J. Cell Biol.* 105:29–39.
- Mimura, N., and A. Asano. 1987. Further characterization of a conserved actin-binding 27-kDa fragment of actinogelin and alpha-actinins and mapping of their binding sites on the actin molecule by chemical cross-linking. *J. Biol. Chem.* 262:4717–4723.

- Ohtsu, M., N. Sakai, H. Fujita, M. Kashiwagi, S. Gasa, S. Shimizu, Y. Eguchi, Y. Tsujimoto, Y. Sakiyama, K. Kobayashi, and N. Kuzumaki. 1997. Inhibition of apoptosis by the actin-regulatory protein gelsolin. *EMBO J.* 16:4650–4656.
- Orlova, A., E. Prochniewicz, and E. H. Egelman. 1995. Structural dynamics of F-actin. II. Cooperativity in structural transitions. *J. Mol. Biol.* 245:598–607.
- Owen, C., and D. DeRosier. 1993. A 13 Å map of the actin-scruiin filament from the *Limulus* acrosomal process. *J. Cell Biol.* 123:337–344.
- Patowski, A., J. Seils, H. Hinssen, and T. Dorfmueller. 1990. Size, shape parameters, and calcium-induced conformational change of the gelsolin molecule: a dynamic light scattering study. *Biopolymers.* 30:427–435.
- Pope, B., S. Maciver, and A. Weeds. 1995. Localization of the calcium-sensitive actin monomer binding site in gelsolin to segment 4 and identification of calcium binding sites. *Biochemistry.* 34:1583–1588.
- Pope, B., M. Way, and A. G. Weeds. 1991. Two of the three actin-binding domains of gelsolin bind to the same subdomain of actin. *FEBS Lett.* 280:70–74.
- Prochniewicz, E., Q. Zhang, P. A. Janmey, and D. D. Thomas. 1996. Cooperativity in F-actin: binding of gelsolin at the barbed end affects structure and dynamics of the whole filament. *J. Mol. Biol.* 260:756–766.
- Rayment, I., H. M. Holden, M. Whittaker, M. Yohn, M. Lorenz, K. C. Holmes, and R. A. Milligan. 1993. Structure of the actin-myosin complex and its implications for muscle contraction. *Science.* 261:58–65.
- Rouayrenc, J. F., A. Fattoum, C. Mejean, and R. Kassab. 1986. Characterization of the calcium-induced conformational changes in gelsolin and identification of interaction regions between actin and gelsolin. *Biochemistry.* 13:3859–3867.
- Schmid, M. F., J. M. Agris, J. Jakana, P. Matsudaira, and W. Chiu. 1994. Three-dimensional structure of a single filament in the *Limulus* acrosomal bundle: scruiin binds to homologous helix-loop-beta motifs in actin. *J. Cell Biol.* 124:341–350.
- Schnuchel, A., R. Wiltscheck, L. Eichinger, M. Schleicher, and T. A. Holak. 1995. Structure of severin domain 2 in solution. *J. Mol. Biol.* 247:21–27.
- Schroder, R. R., D. J. Manstein, W. Jahn, H. Holden, I. Rayment, K. C. Holmes, and J. A. Spudich. 1993. Three-dimensional atomic model of F-actin decorated with Dictyostelium myosin S1. *Nature.* 364:171–174.
- Schroeter, J. P., and J.-P. Breaudiere. 1996. SUPRIM: easily modified image processing software. *J. Struct. Biol.* 116:131–137.
- Sheils, C. A., J. Kas, W. Travassos, P. G. Allen, P. A. Janmey, M. E. Wohl, and T. P. Stossel. 1996. Actin filaments mediate DNA fiber formation in chronic inflammatory airway disease. *Am. J. Pathol.* 148:919–927.
- Spudich, J. A., and S. Watt. 1971. The regulation of rabbit skeletal muscle contraction. I. Biochemical studies of the interaction of the tropomyosin-troponin complex with actin and the proteolytic fragments of myosin. *J. Biol. Chem.* 246:4866–4871.
- Stokes, D. L., and D. J. DeRosier. 1987. The variable twist of actin and its modulation by actin-binding proteins. *J. Cell Biol.* 104:1005–1017.
- Stossel, T. P. 1994a. The E. Donnell Thomas Lecture, 1993. The machinery of blood cell movements. *Blood.* 84:367–379.
- Stossel, T. P. 1994b. Gelsolin: another potential therapy for CF sputum! *CFRI News.* Fall: article 40 (CFRI, Palo Alto, CA).
- Vasconcellos, C. A., P. J. Allen, M. E. Wohl, J. M. Drazen, P. A. Janmey, and T. P. Stossel. 1994. Reduction in viscosity of cystic fibrosis sputum in vitro by gelsolin. *Science.* 263:969–971.
- Vibert, P., R. Craig, and W. Lehman. 1993. Three-dimensional reconstruction of caldesmon-containing smooth muscle filaments. *J. Cell Biol.* 123:313–321.
- Way, M., J. Gooch, B. Pope, and A. G. Weeds. 1989. Expression of human plasma gelsolin in *Escherichia coli* and dissection of actin binding sites by segmental deletion mutagenesis. *J. Cell Biol.* 109:593–605.
- Way, M., B. Pope, and A. G. Weeds. 1992. Evidence for functional homology in the F-actin binding domains of gelsolin and alpha-actinin: implications for the requirements of severing and capping. *J. Cell Biol.* 119:835–842.
- Way, M., and A. Weeds. 1988. Nucleotide sequence of pig plasma gelsolin. Comparison of protein sequence with human gelsolin and other actin-severing proteins shows strong homologies and evidence for large internal repeats. *J. Mol. Biol.* 203:1127–1133.
- Weeds, A. G., and S. Maciver. 1993. F-actin capping proteins. *Curr. Opin. Cell Biol.* 5:63–69.
- Whittaker, M., B. O. Carragher, and R. A. Milligan. 1995b. PHOELIX: a package for automated helical reconstruction. *Ultramicroscopy.* 58:245–260.
- Whittaker, M., E. M. Wilson-Kubalek, J. E. Smith, L. Faust, R. A. Milligan, and H. L. Sweeney. 1995a. A 35-Å movement of smooth muscle myosin on ADP release. *Nature.* 378:748–751.
- Witke, W., A. H. Sharpe, J. H. Hartwig, T. Azuma, T. P. Stossel, and D. J. Kwiatkowski. 1995. Hemostatic, inflammatory, and fibroblast responses are blunted in mice lacking gelsolin. *Cell.* 81:41–51.
- Xian, W., R. Vegners, P. A. Janmey, and W. H. Braunlin. 1995. Spectroscopic studies of phosphoinositide-binding peptide from gelsolin: behavior in solutions of mixed solvent and anionic micelles. *Biophys. J.* 69:2695–2702.
- Yin, H. L., K. Iida, and P. A. Janmey. 1988. Identification of a polyphosphoinositide-regulated actin-modulated domain in gelsolin which binds to the sides of actin filaments. *J. Cell Biol.* 106:805–812.
- Yin, H. L., and T. P. Stossel. 1979. Control of cytoplasmic actin gel-sol transformation by gelsolin, a calcium-dependent regulatory protein. *Nature.* 281:585–586.
- Zhou, Z. H., S. Hardt, B. Wang, M. B. Sherman, J. Jakana, and W. Chiu. 1996. CTF determination of images of ice-embedded single particles using a graphics interface. *J. Struct. Biol.* 116:216–223.